Effect of the Wood-Saxon nucleon distribution on the chiral magnetic field in relativistic heavy-ion collisions

Yu-Jun Mo,[1,2] Sheng-Qin Feng,[1,2,3] and Ya-Fei Shi[1]
[1]*College of Science, Three Gorges University, Yichang 443002, China*
[2]*Key Laboratory of Quark and Lepton Physics (Huazhong Normal University), Ministry of Education, Wuhan 430079, China*
[3]*School of Physics and Technology, Wuhan University, Wuhan 430072, China*
(Received 13 January 2013; revised manuscript received 28 May 2013; published 2 August 2013)

The formation of the QCD vacuum with nonzero winding number Q_w during relativistic heavy-ion collisions breaks the parity and charge-parity symmetry. A new kind of field configuration can separate charge in the presence of a background magnetic field—the "chiral magnetic effect." The strong magnetic field and the QCD vacuum can both completely be produced in the noncentral nuclear-nuclear collision. Based on the theory of Kharzeev, McLerran, and Warringa, we use the Wood-Saxon nucleon distribution to replace that of the uniform distribution to improve the magnetic field calculation method of the noncentral collision. The chiral magnetic field distribution at Large Hadron Collider (LHC) energy regions are predicted. We also calculate the contributions to the magnetic field of the total charge given by produced quarks.

DOI: 10.1103/PhysRevC.88.024901 PACS number(s): 25.75.Ld, 11.30.Er, 11.30.Rd

I. INTRODUCTION

When two heavy ions collide with a nonzero impact parameter, a magnetic (electromagnetic) field of enormous magnitude is created in the direction of angular momentum of the collision [1–3]. If a nonzero chirality is present in such a situation, an electromagnetic current will be induced in the direction of the magnetic field. This is the so-called chiral magnetic effect [4–6].

One of the most exciting signals of the deconfinement and the chiral phase transitions in heavy-ion collisions, the chiral magnetic effect [7–12], predicts the preferential emission of charged particles along the direction of angular momentum in the case of noncentral heavy-ion collisions due to the presence of nonzero chirality. As it was stressed in Refs. [1–3], both the deconfinement and the chiral phase transitions are essential requirements for the chiral magnetic effect to take place.

In a heavy-ion collision this current leads to an excess of positive charge on one side of the reaction plane (the plane in which the beam axis and the impact parameter lies) and negative charge on the other; the resulting charge asymmetry is also modulated by the radial flow and the transport properties of the medium. This charge asymmetry can be investigated experimentally [13–17] using the observable proposed [18–21].

In recent years, Kharzeev, McLerran, and Warringa (KMW) presented new evidence of a charge-parity (CP) violation in relativistic heavy-ion collisions caused by the nonzero Q_w gauge field configurations [1,2]. KMW proposed that this kind of configuration can separate charge, which means the right- and left-hand quarks created during the collisions will move oppositely with respect to the reaction plane in the presence of a background magnetic field. Also, high-energy physics experiments have obtained a series of results to support the chiral magnetic effect.

KMW [1] presented a novel mechanism for charge separation. The topological charge changing transitions provide the parity (P) and CP violations necessary for charge separation. The variance of the net topological charge change is proportional to the total number of topological charge changing transitions. Hence, if sufficiently hot matter is created in heavy-ion collisions so that topological charge transitions can take place, we expect on average in each event a finite amount of topological charge change.

Charge separation needs a symmetry axis along which the separation can take place. The only symmetry axis in a heavy-ion collision is angular momentum, which points in the direction perpendicular to the reaction plane. In central collisions there is no symmetry axis, so in that case charge separation should vanish. The strong magnetic field and the QCD vacuum can both completely be produced in the noncentral nuclear-nuclear collision. Based on the theory of KMW, we use the Wood-Saxon nucleon distribution to replace that of the uniform distribution to improve the magnetic field calculation method of the noncentral collision. The chiral magnetic field distribution at Large Hadron Collider (LHC) energy regions are predicted in this paper.

The paper is organized as follows. The modified calculation of chiral magnetic field and the comparison of our results with that given by KMW are described in Sec. II, along with the predicted results of the LHC energy region. The produced particle contribution to the magnetic field is considered in Sec. III. A summary is given in Sec. IV.

II. THE MODIFIED CALCULATION OF CHIRAL MAGNETIC FIELD

The situation with the experimental search for the local strong parity violation drastically changed once it was noticed [1–6] that in noncentral nuclear collisions it would lead to asymmetry in the emission of positively and negatively charged particles perpendicular to the reaction plane. Such a charge separation is a consequence of the difference in the number of quarks with positive and negative helicities positioned in the strong magnetic field of a noncentral nuclear collision, the so-called chiral magnetic effect (CME).

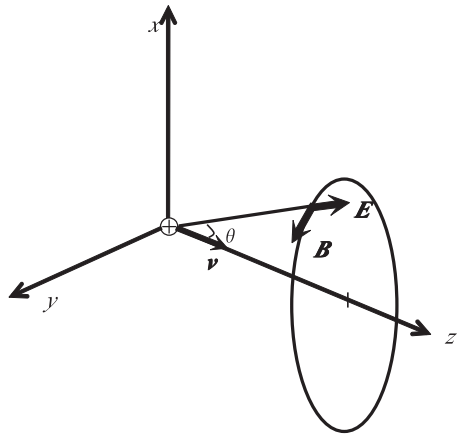

FIG. 1. The magnetic field around a moving charged particle.

We begin with a charged particle moving along the direction of the z axis as shown in Fig. 1. The magnetic field around it can be given by

$$\vec{B} = \frac{1}{c^2}\vec{v} \times \vec{E}. \tag{1}$$

If the movement is relativistic, at the time $t = 0$, the charge is the origin of the coordinates. The magnitude of the magnetic field $\vec{B}$ is given by

$$B = \frac{1}{4\pi\varepsilon_0 c^2}\frac{qv(1-\beta^2)\sin\theta}{r^2(1-\beta^2\sin\theta)^{3/2}}. \tag{2}$$

Now we consider a particle with charge Z and rapidity Y traveling along the z axis. At $t = 0$ the particle can be found at position $\vec{x}'_\perp$; the magnetic field at the position $\vec{x} = (\vec{x}_\perp, z)$ caused by the particle is given by

$$e\vec{B}(\vec{x}) = Z\alpha_{EM}\sinh Y \times \frac{(\vec{x}'_\perp - \vec{x}_\perp)\times\vec{e}_z}{[(\vec{x}'_\perp - \vec{x}_\perp)^2 + (t\sinh Y - z\cosh Y)^2]^{3/2}}. \tag{3}$$

Now we suppose two similar nuclei with charge Z and radius R are traveling in positive and negative z directions with rapidity Y_0. At $t = 0$ they have a noncentral collision with impact parameter b at the origin point. We take the centers of the two nuclei at $x = \pm b/2$ at time $t = 0$ so that the direction of b lies along the x axis (see Fig. 2).

As the nuclei are nearly traveling with the speed of light in typical heavy-ion collision experiments, the Lorentz contraction factor γ is so large that we can consider the two included nuclei as pancake shaped. As a result, the nucleon's number density of each nuclei at $\vec{x}' = (\vec{x}'_\perp, z)$ can be given by

$$\rho_{s\pm}(\vec{x}'_\perp) = \frac{2}{4/3\pi R^3}\sqrt{R^2 - (\vec{x}'_\perp \pm \vec{b}/2)^2}. \tag{4}$$

As a result, it seems that the nucleon distribution on average in a nucleus is an approximate result before considering the Lorentz contraction. In Ref. [1], the KMW model used the uniform nuclear distribution as the nuclear distribution. But for a real situation, the nucleon distribution is not strictly uniform. It seems more reasonable to use the Wood-Saxon distribution

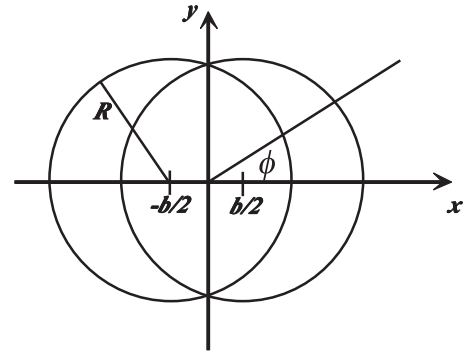

FIG. 2. Cross-sectional view of a noncentral heavy-ion collision along the z axis. The two nuclei have radii R, move in opposite directions, and collide with impact parameter b. The plane $y = 0$ is called the reaction plane. The angle ϕ is an azimuthal angle with respect to the reaction plane. The region in which the two nuclei overlap contains the participants; the regions in which they do not overlap contain the spectators.

to replace the uniform distribution. We use the Wood-Saxon distribution in this paper,

$$n_A(r) = \frac{n_0}{1+\exp\left(\frac{r-R}{d}\right)}, \tag{5}$$

where $n_0 = 0.17\ \mathrm{fm}^{-3}$, $d = 0.54$ fm, and the radius $R = 1.12\,A^{1/3}$ fm. Considering the Lorentz contraction, the density in the two-dimensional plane can be given by

$$\rho_\pm(\vec{x}'_\perp) = N\int_{-\mathrm{R}}^{\mathrm{R}} dz' \frac{n_0}{1+\exp\left(\frac{\sqrt{(x'\mp b/2)^2+y'^2+z'^2}-\mathrm{R}}{d}\right)}, \tag{6}$$

where N is the normalization constant. The number densities should be normalized as

$$\int d\vec{x}'_\perp \rho_\pm(\vec{x}'_\perp) = 1. \tag{7}$$

We now estimate the strength of the magnetic field at position $\vec{x} = (\vec{x}_\perp, z)$ caused by the two traveling nuclei. We are only interested in the time $t > 0$, i.e., just after the collision. Then we can split the contribution of particles to the magnetic field in the following way:

$$\vec{B} = \vec{B}_s^+ + \vec{B}_s^- + \vec{B}_p^+ + \vec{B}_p^-, \tag{8}$$

where $\vec{B}_s^\pm$ and $\vec{B}_p^\pm$ are the contributions of the spectators and the participants moving in the positive or negative z direction, respectively. For spectators, we assume that they do not scatter at all and that they keep traveling with the beam rapidity Y_0. According to Eq. (3), we use the density above and find

$$e\vec{B}_s^\pm(\tau,\eta,\vec{x}_\perp) = \pm Z\alpha_{EM}\sinh(Y_0\mp\eta)\int d^2\vec{x}'_\perp\rho_\pm(\vec{x}'_\perp) \times[1-\theta_\mp(\vec{x}'_\perp)]\frac{(\vec{x}'_\perp-\vec{x}_\perp)\times\vec{e}_z}{[(\vec{x}'_\perp-\vec{x}_\perp)^2+\tau^2\sinh(Y_0\mp\eta)^2]^{3/2}}, \tag{9}$$

where $\tau = (t^2 - z^2)^{1/2}$ is the proper time, $\eta = \frac{1}{2}\ln[(t+z)/(t-z)]$ is the space-time rapidity, and

$$\theta_{\mp}(\vec{x}'_{\perp}) = \theta[R^2 - (\vec{x}'_{\perp} \pm \vec{b}/2)^2]. \tag{10}$$

Here, we would like to neglect the contribution of the production particles created by the interactions approximately and so we just need to take into account the contribution of the participants that were originally there. The distribution of participants that remain traveling along the beam axis is given by

$$f(Y) = \frac{a}{2\sinh(aY_0)} e^{aY}, \quad -Y_0 \leqslant Y \leqslant Y_0. \tag{11}$$

Experimental data show that $a \approx 1/2$, consistent with the baryon junction stopping mechanism. The contribution of the participants to the magnetic field can be also given by

$$\begin{aligned} &e\vec{B}_p^{\pm}(\tau, \eta, \vec{x}_{\perp}) \\ &= \pm Z\alpha_{EM} \int d^2\vec{x}'_{\perp} \int dY f(Y) \sinh(Y \mp \eta) \\ &\quad \times \rho_{\pm}(\vec{x}'_{\perp})\theta_{\mp}(\vec{x}'_{\perp}) \frac{(\vec{x}'_{\perp} - \vec{x}_{\perp}) \times \vec{e}_z}{[(\vec{x}'_{\perp} - \vec{x}_{\perp})^2 + \tau^2 \sinh(Y \mp \eta)^2]^{\frac{3}{2}}}. \end{aligned} \tag{12}$$

We calculate the magnetite of the magnetic field at the origin ($\eta = 0, \vec{x}_{\perp} = 0$), in which case it is pointing in the y direction. We took a Au-Au collision with different beam rapidities and different impact parameters.

Figure 3 shows the dependence of the magnetic field on the proper time for a Au-Au collision with $b = 8$ fm at $\sqrt{s} =$ 64 GeV. The solid line denotes our calculation results using the Wood-Saxon nuclear distribution, and the dashed line denotes

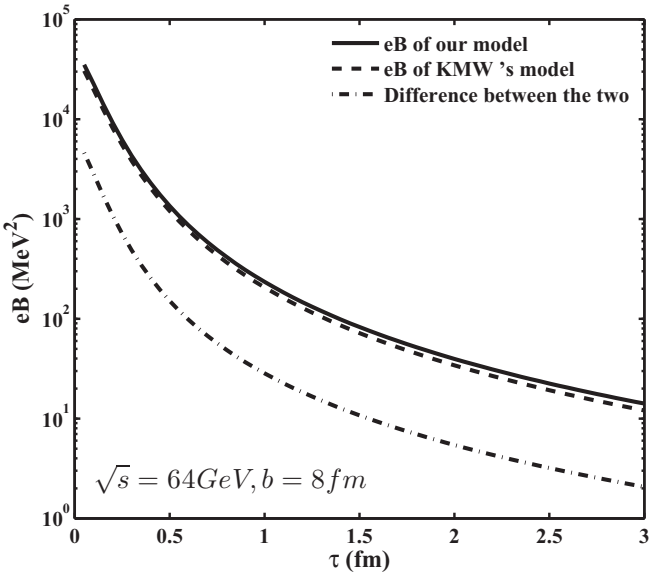

FIG. 3. The dependence of the magnetic field on proper time for Au-Au collisions with $\sqrt{s} = 64$ GeV and $b = 8$ fm. The solid line denotes our calculation results by using the Wood-Saxon nuclear distribution, the dashed line denotes the KMW results by using the uniform nuclear distribution, and the dash-dotted line denotes the difference between our model and KMW's model.

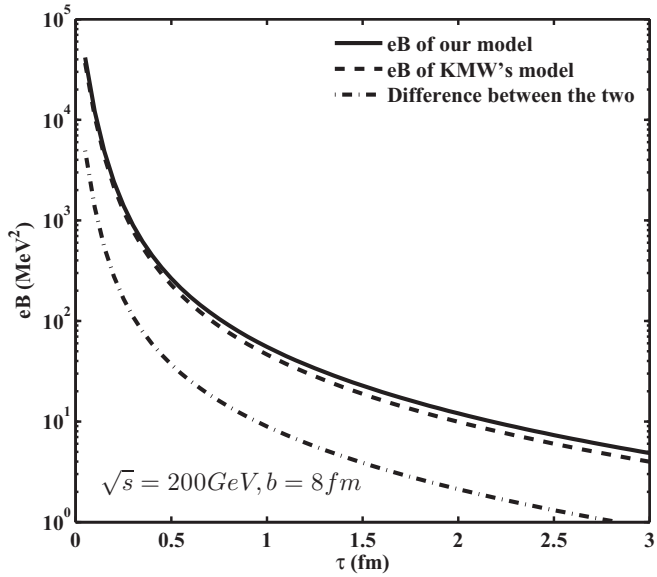

FIG. 4. The same as Fig. 3 but for $\sqrt{s} = 200$ GeV.

the KMW results using the uniform nuclear distribution. The dash-dotted line is the difference between our model and KMW's model. From Fig. 3 we know that the magnetic fields can indeed be created in noncentral heavy-ion collisions and it is this field that makes it possible to separate the right- and left-hand quarks. Figures 3 and 4 also show that the size of the field is quite large, especially just after the collision, and decreases rapidly over time, and the magnitude of the magnetic field using the Wood-Saxon nuclear distribution is slightly bigger that that using the uniform distribution. Figure 4 shows the dependence of the magnetic field on proper time for a Au-Au collision with $b = 8$ fm and $\sqrt{s} = 200$ GeV. The same situation is also shown in Fig. 3.

Figure 5 shows the dependencies of the magnetic field on proper time for Au-Au collisions at different collision energies $\sqrt{s} = 64$ GeV [Fig. 5(a)] and $\sqrt{s} = 200$ GeV [Fig. 5(b)], respectively. Figure 5(a) shows us that the magnetic field is slightly large for large impact parameter b when $\tau \leqslant 1.2$ fm at $\sqrt{s} = 64$ GeV, and $\tau \sim 1.2$ fm is a cross point. But when $\tau > 1.2$ fm, the magnetic field is relatively larger for small impact parameter b than it is for the large impact parameter. Figure 5(b) shows that when the energy of the center-of-mass central system increases from $\sqrt{s} = 64$ GeV to $\sqrt{s} =$ 200 GeV, the magnetic fields are nearly unchanged when $\tau \leqslant 0.3$ fm, and $\tau \sim 0.3$ fm is a cross point. The magnitude of the cross point at $\sqrt{s} = 200$ GeV is far less than that at $\sqrt{s} = 64$ GeV. When $\tau > 0.3$ fm, the magnetic field is relatively large for small impact parameter b.

Figure 6 shows the dependencies of the magnetic field on proper time for Au-Au collisions at different impact parameters of $b = 4$ fm [Fig. 6(a)] and $b = 8$ fm [Fig. 6(b)], respectively. Figures 6(a) and 6(b) show us that the magnetic field at $\sqrt{s} = 64$ GeV is larger than that at $\sqrt{s} = 200$ GeV.

We have done further research based on the discussion above. The magnetic field at the LHC energy regions is predicted by using Eqs. (9) and (12). Figure 7 shows the dependencies of the magnetic field on proper time for Pb-Pb

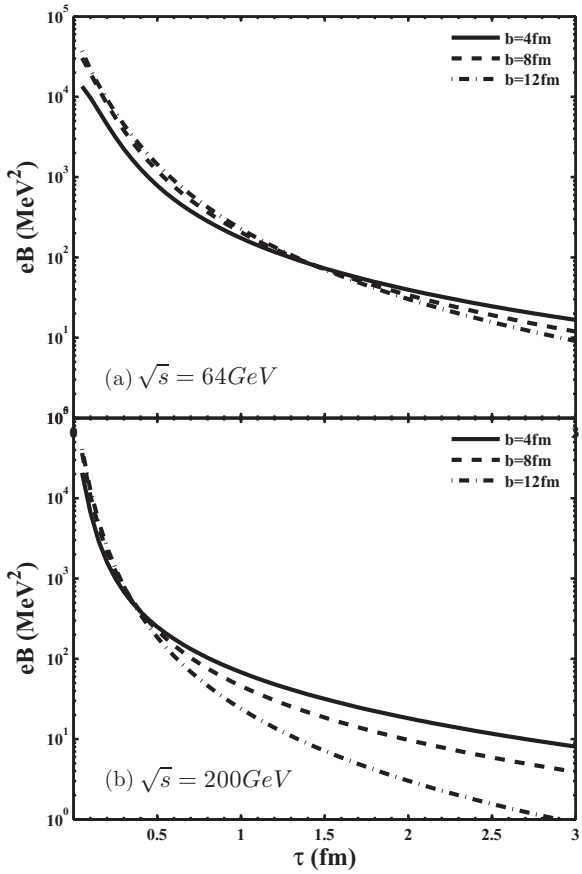

FIG. 5. The dependencies of the magnetic field on proper time for Au-Au collisions at different collision energies for (a) $\sqrt{s} = 64$ GeV and (b) $\sqrt{s} = 200$ GeV.

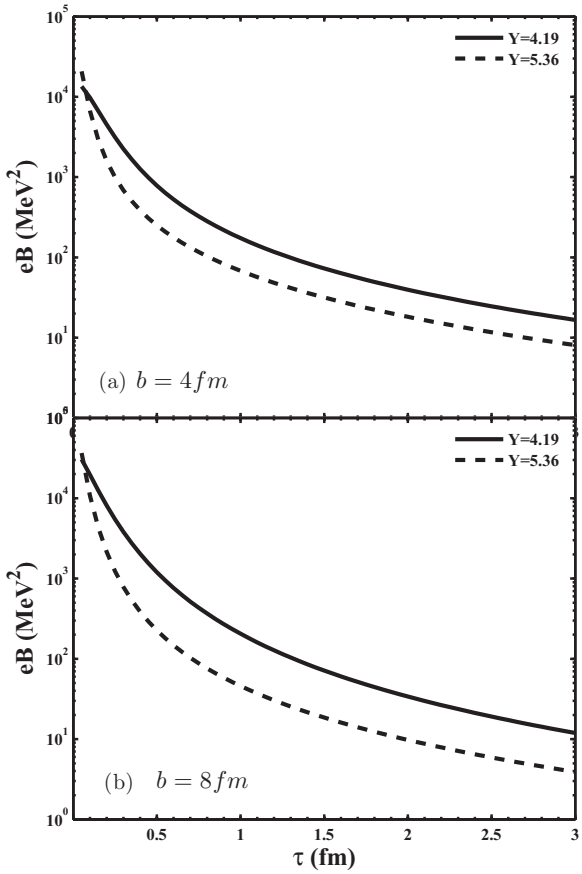

FIG. 6. The dependencies of the magnetic field on proper time for Au-Au collisions at different impact parameters of (a) $b = 4$ fm and (b) $b = 8$ fm.

collisions and $\sqrt{s} = 900$ GeV at different impact parameters of $b = 4$, $b = 8$, and $b = 12$ fm, respectively. Figure 7 shows that, at $\tau \sim 0$, the magnitudes of the magnetic field at $b = 4$, $b = 8$, and $b = 12$ fm are nearly same, but the magnitudes of the magnetic field decrease as τ increases. It is shown that the magnitudes of the magnetic field of more off-central collisions ($b = 12$ fm) drop dramatically along with the time. We also predict the dependencies of a magnetic field on proper time for Pb-Pb collisions and $\sqrt{s} = 2760$ GeV (Fig. 8) and at $\sqrt{s} = 5500$ GeV (Fig. 9), respectively. Figures 8 and 9 present the same rule as in Fig. 7. It is obvious that the magnitude of the magnetic field in the LHC energy region is not as big as the ones in the Relativistic Heavy Ion Collider (RHIC) energy regions.

The analysis shows an enormous magnetic field can indeed be created in off-central heavy-ion collisions and it is this field that makes it possible to separate the right- and left-hand quarks. The size of the field is quite large, especially just after the collision, and decreases rapidly over time.

III. THE MAGNETIC FIELD OF TOTAL CHARGES BY THE PRODUCED QUARKS

To discuss the produced quark distribution, we start with the momentum spectrum of quarks radiated by a stationary thermal source with temperature $T_{\rm th}$:

$$E\frac{d^3N_{\rm th}}{d^3p} = \frac{d^3N_{\rm th}}{dYdp_Td\phi} \propto Ee^{-E/T_{\rm th}}. \tag{13}$$

In the following we give the spectra in terms of rapidity $Y = \tanh^{-1}(p_{L/E})$. The rapidity distribution of thermal quarks can be given by integrating Eq. (13) over the transverse component [22,23], such as

$$\frac{dN_{\rm th}}{dY} \propto \frac{mT_{\rm th}}{(2\pi)^2}\left(1 + 2\xi_0 + 2\xi_0^2\right)e^{(-1/\xi_0)}, \tag{14}$$

where $\xi_0 = T_{\rm th}/(m\cosh Y)$.

Equations (13) and (14) give the isotropic thermal distribution. As mentioned in Refs. [24–27], the measured momentum distribution of the produced particles is certainly anisotropic [28–37]. It is privileged in the direction of the incident nuclei. This is because the produced particles still carry their kinematic information, making the longitudinal direction more populated than the transverse ones. The simplest way [22,23,28] to account for the anisotropy is to add up the contributions from a set of fireballs with centers located uniformly in the rapidity region $[-Y_{f0}, Y_{f0}]$. The corresponding rapidity distribution is obtained through changing ξ_0 into $\xi = T_{\rm th}/[m\cosh(Y - Y_f)]$ and integrating

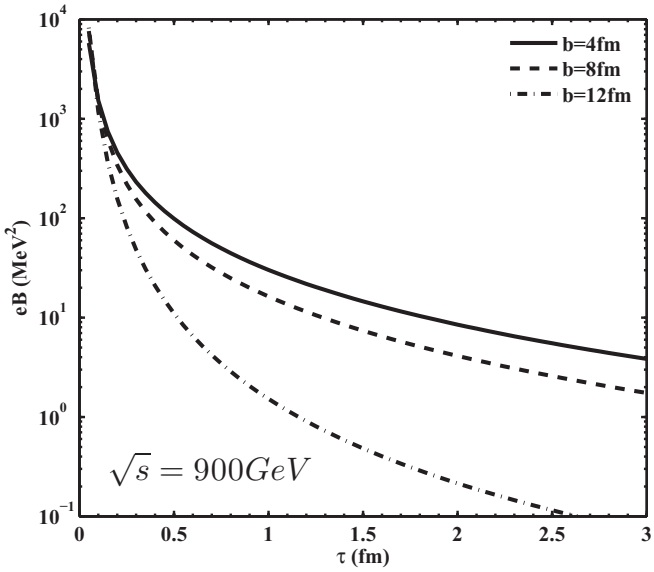

FIG. 7. The dependencies of the magnetic field on proper time for Pb-Pb collisions and $\sqrt{s} = 900$ GeV at different impact parameters of $b = 4$, $b = 8$ and $b = 12$ fm.

over Y_f from $-Y_{f0}$ to Y_{f0}:

$$\frac{dN_{\rm th}}{dY} \propto \int_{-Y_{f0}}^{Y_{f0}} dY_f \frac{mT_{\rm th}}{(2\pi)^2}(1 + 2\xi + 2\xi^2)e^{(-1/\xi)}, \tag{15}$$

where $\xi = T_{\rm th}/[m\cosh(Y - Y_f)]$. The distribution of produced quarks can be given by

$$f(Y) = K\int_{-Y_{f0}}^{Y_{f0}} (1 + 2\Gamma + 2\Gamma^2)e^{-1/\Gamma} dY_f. \tag{16}$$

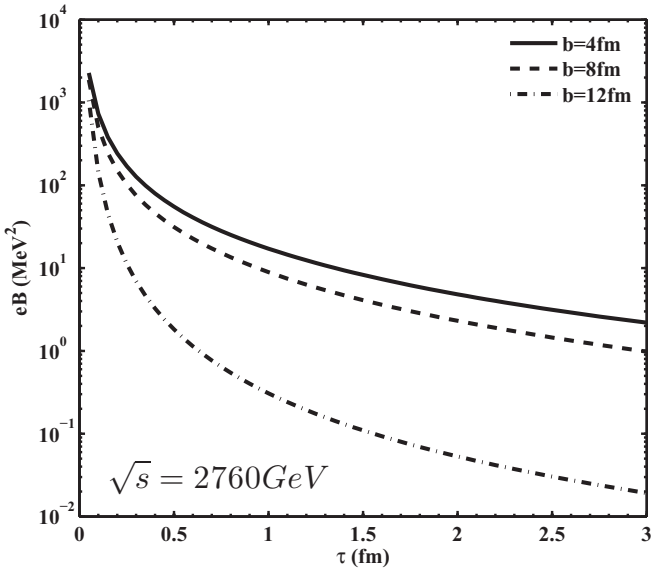

FIG. 8. The dependencies of the magnetic field on proper time for Pb-Pb collisions and $\sqrt{s} = 2760$ GeV at different impact parameters of $b = 4$, $b = 8$, and $b = 12$ fm.

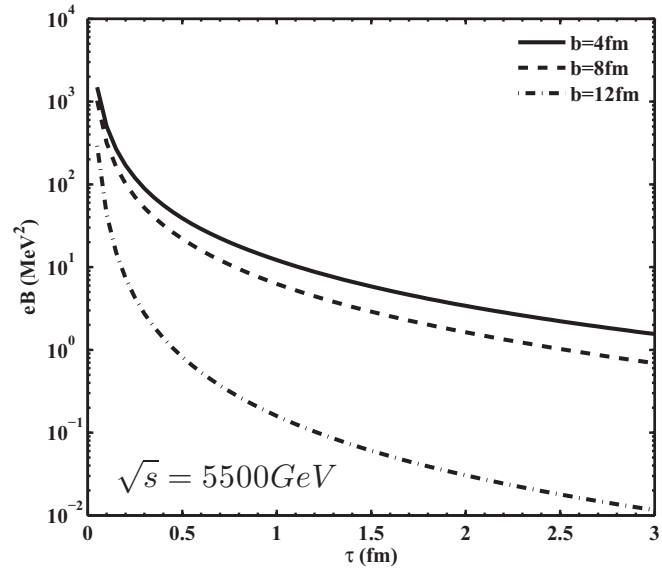

FIG. 9. The same as Fig. 8 but for $\sqrt{s} = 5500$ GeV.

It also should be normalized and K is a normalization constant. Here

$$\Gamma = \frac{T_{\rm th}e^{-(\tau-\tau_0)/\tau_0}}{m\cosh(Y - Y_f)}. \tag{17}$$

Let us try to figure out how the density of the electric charge should be dependent on the chemical potential and the nucleon number of colliding nuclei:

$$\rho_{q\pm}(\vec{x}'_\perp, Y) = \kappa\frac{\rho_\pm(\vec{x}'_\perp)}{1 + \exp\left(\frac{\varepsilon(Y)-\mu_q}{T}\right)}, \tag{18}$$

where $\varepsilon(Y)$ is the quark energy as a function of the rapidity Y of produced quarks, μ_q is the quark chemical potential, T is temperature, and κ is a normalization constant. The energy of the quark is given as

$$\varepsilon(Y) = \sqrt{m^2 + p_{\rm T}^2}\cosh Y, \tag{19}$$

where we assume the average transverse momentum $p_{\rm T} = 0.2$ GeV, the constituent quark mass $m = 0.308$ GeV, and the temperature $T = 0.2$ GeV. With the parametrizations of T and baryon chemical potential μ_B from Fig. 1 of Ref. [38], we assume that $\mu_B = 0.03$ GeV with $\mu_q = 0.01$ GeV at $\sqrt{s} = 200$ GeV, and $\mu_B = 0.06$ GeV with $\mu_q = 0.02$ GeV at $\sqrt{s} = 64$ GeV.

Then we get the expression for the magnetic field of the total charge given by the produced particles:

$$\begin{aligned} e\vec{B}(\tau, \eta, \vec{x}_\perp) &= \pm ZK\alpha_{EM}\int d^2\vec{x}'_\perp \int dY \int_{-Y_{f0}}^{Y_{f0}} dY_f \\ &\times (1 + 2\Gamma + 2\Gamma^2)e^{-1/\Gamma}\sinh(Y \mp \eta) \\ &\times \rho_{q\pm}(\vec{x}'_\perp, Y)\frac{(\vec{x}'_\perp - \vec{x}_\perp)\times\vec{e}_z}{[(\vec{x}'_\perp - \vec{x}_\perp)^2 + \tau^2\sinh(Y \mp \eta)^2]^{\frac{3}{2}}}. \end{aligned} \tag{20}$$

Figure 10 shows the dependence of the magnetic field on the total charge given by produced particles at proper time for

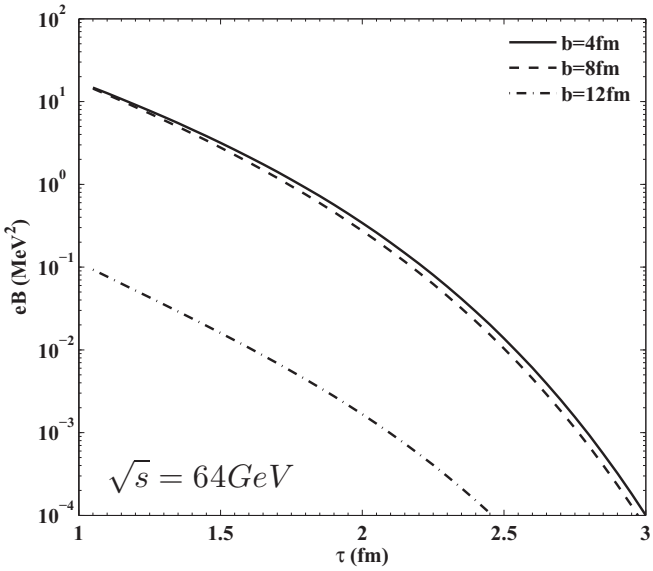

FIG. 10. The dependence of the magnetic field of total charge given by the produced particles on proper time for Au-Au collision with $\sqrt{s} = 64$ GeV at $b = 4$, $b = 8$, and $b = 12$ fm.

a Au-Au collision with $\sqrt{s} = 64$ GeV at $b = 4$, $b = 8$, and $b = 12$ fm, respectively. The solid line is for $b = 4$ fm, the dashed line is for $b = 8$ fm, and the dash-dotted line is for $b = 12$ fm. Equation (18) is used to calculate the results of produced particles. From Eq. (18), as a whole, we can figure out that the contribution to the magnetic field of produced particles is smaller than that of contributions of participant and spectator nucleons. A smaller impact parameter results in a larger magnitude of produced particles. When $b \to 12$ fm, the magnitude of the magnetic field of produced particles is approximately 0.

Figure 11 shows the dependence of the magnetic field on the total charge given by produced particles at proper time for a Au-Au collision with $\sqrt{s} = 200$ GeV at $b = 4$, $b = 8$, and $b = 12$ fm, respectively.

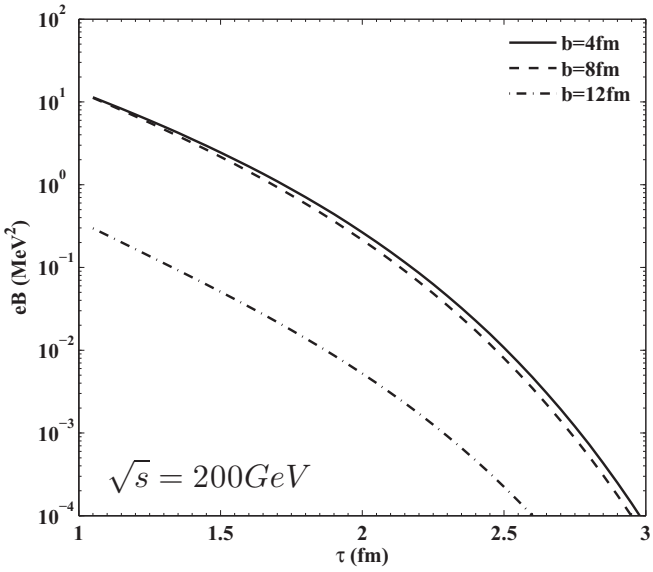

FIG. 11. The same as Fig. 10 but for $\sqrt{s} = 200$ GeV.

IV. SUMMARY AND CONCLUSION

In this paper, we start from the magnetic field produced by traveling charged particles and estimate the magnetic field in a reasonable way with the Wood-Saxon distribution instead of the model of uniform distribution in nuclei. We acquired useful results at the same time.

The QCD vacuum with nonzero winding number Q_w, which is created in heavy-ion collisions, breaks the CP symmetry. As a result, we obtain a difference between the number of left- and right-handed fermions for each flavor. In the presence of a background magnetic field B which is also created in heavy-ion collision, the right- and left-handed fermions move oppositely and then a charge difference between opposite sides of the reaction plane is induced. This is the chiral magnetic effect. This kind of charge difference has been indeed observed in high-energy physics experiments and the phenomenon can be used as a proof of CP violation. We can also use the magnetic field we have and another model to estimate this kind of effect theoretically.

We show that an enormous magnetic field can indeed be created in off-central heavy-ion collisions. It is shown that this magnetic field makes it possible to separate the right- and left-hand quarks. The magnitude of the field is quite large, especially just after the collision, and decreases rapidly with time. The drop velocity increases with the collision energy increase. It is shown that the magnitudes of the magnetic field of more off-central collision at the LHC energy region drop dramatically along with the time. We also predict the dependencies of the magnetic field on proper time for Pb-Pb collisions at $\sqrt{s} = 2760$ and $\sqrt{s} = 5500$ GeV (Fig. 9), respectively.

We also show the dependence of the magnetic field of the total charge given by the produced quarks on proper time for a Au-Au collision with $\sqrt{s} = 64$ GeV and $\sqrt{s} = 200$ GeV at $b = 4$, $b = 8$, and $b = 12$ fm, respectively. It is shown that the contribution to the magnetic field of the total charge given by the produced quarks is smaller than that of contributions of participant and spectator nucleons. We also find that the magnitude of the magnetic field given by produced quarks increases with the impact parameter decreases.

ACKNOWLEDGMENTS

This work was supported by the National Natural Science Foundation of China (Grant No. 10975091), the CCNU-QLPL Innovation Fund (Grant No. QLPL2011P01), the Excellent Youth Foundation of Hubei Scientific Committee (Grant No. 2006ABB036), and the Education Commission of Hubei Province of China (Grant No. Z20081302). The authors are indebted to Professor Lianshou Liu for his valuable discussions and very helpful suggestions.

[1] D. E. Kharzeev, L. D. McLerran, and H. J. Warringa, Nucl. Phys. A **803**, 227 (2008).
[2] V. Skokov, A. Illarionov, and V. Toneev, Int. J. Mod. Phys. A **24**, 5925 (2009).
[3] H. Minakata and B. Muller, Phys. Lett. B **377**, 135 (1996).
[4] D. Kharzeev, Phys. Lett. B **633**, 260 (2006).
[5] D. Kharzeev and A. Zhitnitsky, Nucl. Phys. A **797**, 67 (2007).
[6] K. Fukushima, D. E. Kharzeev, and H. J. Warringa, Phys. Rev. D **78**, 074033 (2008).
[7] Y. Burnier, D. E. Kharzeev, J. Liao, and H. U. Yee, Phys. Rev. Lett. **107**, 052303 (2011).
[8] D. E. Kharzeev and D. T. Son, Phys. Rev. Lett. **106**, 062301 (2011).
[9] G. Basar, G. V. Dunne, and D. E. Kharzeev, Phys. Rev. Lett. **104**, 232301 (2010).
[10] K. Fukushima, D. E. Kharzeev, and H. J. Warringa, Phys. Rev. Lett. **104**, 212001 (2010).
[11] K. Fukushima, D. E. Kharzeev, and H. J. Warringa, Nucl. Phys. A **836**, 311 (2010).
[12] H. J. Warringa, Phys. Rev. D **86**, 085029 (2012).
[13] S. A. Voloshin, Phys. Rev. C **70**, 057901 (2004).
[14] I. V. Selyuzhenkov (STAR Collaboration), Rom. Rep. Phys. **58**, 049 (2006).
[15] S. A. Voloshin (STAR Collaboration), Nucl. Phys. A **830**, 337c (2009).
[16] S. A. Voloshin, Phys. Rev. Lett. **105**, 172301 (2010).
[17] B. I. Abelev *et al*. (STAR Collaboration), Phys. Rev. C **81**, 054908 (2010).
[18] B. I. Abelev *et al*. (STAR Collaboration), Phys. Rev. Lett. **103**, 251601 (2009).
[19] N. N. Ajitanand, Roy A. Lacey, A. Taranenko, and J. M. Alexander, Phys. Rev. C **83**, 011901 (2011).
[20] F. Wang, Phys. Rev. C **81**, 064902 (2010).
[21] M. Asakawa, A. Majumder, and B. Muller, Phys. Rev. C **81**, 064912 (2010).
[22] E. Schnedermann, J. Sollfrank, and U. Heinz, Phys. Rev. C **48**, 2462 (1993).
[23] E. Schnedermann, J. Sollfrank, and U. Heinz, Prog. Part. Nucl. Phys. **30**, 401 (1993).
[24] Feng Shengqin, Liu Feng, and Liu Lianshou, Phys. Rev. C **63**, 014901 (2000).
[25] S. Q. Feng and Y. Zhong, Phys. Rev. C **83**, 034908 (2011).
[26] S. Q. Feng and W. Xiong, Phys. Rev. C **77**, 044906 (2008).
[27] X. Cai, S. Q. Feng, Y. D. Li, C. B. Yang, and D. C. Zhou, Phys. Rev. C **51**, 3336 (1995).
[28] P. Braun-Munzinger, J. Stachel, J. P. Wessels, and N. Xu, Phys. Lett. B **344**, 43 (1995).
[29] P. Braun-Munzinger, I. Heppe, and J. Stachel, Phys. Lett. B **465**, 15 (1999).
[30] F. Becattini, J. Cleymans, A. Keranen, E. Suhonen, and K. Redlich, Phys. Rev. C **64**, 024901 (2001).
[31] J. Cleymans and K. Redlich, Phys. Rev. Lett. **81**, 5284 (1998).
[32] D. H. Rischke, S. Bernard, and J. A. Maruhn, Nucl. Phys. A **595**, 346 (1995).
[33] D. H. Rischke, Y. Pursun, and J. A. Maruhn, Nucl. Phys. A **595**, 383 (1995); **596**, 717(E) (1996).
[34] C. M. Hung and E. V. Shuryak, Phys. Rev. Lett. **75**, 4003 (1995).
[35] P. Huovinen, P. F. Kolb, U. W. Heinz, P. V. Ruuskanen, and S. A. Voloshin, Phys. Lett. B **503**, 58 (2001).
[36] P. F. Kolb, P. Huovinen, U. W. Heinz, and H. Heiselberg, Phys. Lett. B **500**, 232 (2001).
[37] P. F. Kolb, U. W. Heinz, P. Huovinen, K. J. Eskola, and K. Tuominen, Nucl. Phys. A **696**, 197 (2001).
[38] A. Andronic, D. Blaschke, P. Braun-Munzinger, J. Cleymans, K. Fukushima, L. D. McLerran, H. Oeschler, R. D. Pisarski, K. Redlich, C. Sasaki, H. Satz, and J. Stachel, Nucl. Phys. A **837**, 65 (2010).